B061495

NASA TECHNICAL NOTE

NASA TN D-2924

NASA TN D-2924

of

HEAT-TRANSFER AND PRESSURE DROP CORRELATIONS FOR HYDROGEN AND NITROGEN FLOWING THROUGH TUNGSTEN WIRE MESH AT TEMPERATURES TO 5200° R

by Byron L. Siegel, William L. Maag,
Jack G. Slaby, and William F. Mattson

Lewis Research Center
Cleveland, Ohio

NATIONAL AERONAUTICS AND SPACE ADMINISTRATION • WASHINGTON, D. C. • JULY 1965

NASA TN D-2924

HEAT-TRANSFER AND PRESSURE DROP CORRELATIONS FOR HYDROGEN AND NITROGEN FLOWING THROUGH TUNGSTEN WIRE MESH AT TEMPERATURES TO 5200° R

By Byron L. Siegel, William L. Maag, Jack G. Slaby, and William F. Mattson

Lewis Research Center
Cleveland, Ohio

NATIONAL AERONAUTICS AND SPACE ADMINISTRATION

For sale by the Clearinghouse for Federal Scientific and Technical Information
Springfield, Virginia 22151 – Price $2.00

HEAT-TRANSFER AND PRESSURE DROP CORRELATIONS FOR HYDROGEN AND NITROGEN FLOWING THROUGH TUNGSTEN WIRE MESH AT TEMPERATURES TO 5200° R

by Byron L. Siegel, William L. Maag, Jack G. Slaby, and William F. Mattson

Lewis Research Center

SUMMARY

Correlations for variable property heat-transfer and friction pressure drop data were obtained for forced convection of hydrogen and nitrogen through electrically heated tungsten wire mesh. These correlations represent the data of six different helically coiled wire meshes for the following range of conditions:

(1) Mesh porosity of 64 to 72.2 percent

(2) Wire diameter of 0.020 to 0.035 inch

(3) Surface temperature of 1400° to 5200° R

(4) Outlet gas temperature of 600° to 2400° R

(5) Mass velocity for hydrogen of 0.4 to 3.1 lb/(sec)(sq ft) and for nitrogen of 4.5 to 10.2 lb/(sec)(sq ft)

(6) Heat flux of 0.5 to 8.3 Btu/(sec)(sq in.)

(7) Pressure level of 1 atmosphere

The effect of flow bypass, resulting from a mesh heater not filling the flow passage, was investigated on a 0.030-inch-diameter wire mesh for a bypass area of 25 percent. end

INTRODUCTION

The Lewis Research Center is conducting research on a tungsten-water-moderated, hydrogen propelled, nuclear rocket concept. A part of the experimental phase of this program is to evaluate various types of fuel elements and supporting structures at simulated operating conditions

The results of this report were used to design the heating elements of a high-temperature hydrogen preheater for hot flow testing. The prerequisites for these elements were that they must have:

(1) Capability of being electrically heated to surface temperatures of 5500° R

(2) Electrical resistance to match an available high-voltage power supply

(3) Sufficient surface area to transfer the generated heat to the flowing gas

(4) Sufficient flow area to minimize gas pressure drop

Commercially available tungsten mesh made of interwound helical coils of tungsten wire were considered applicable as the heating elements for this preheater, but their heat-transfer and pressure drop characteristics were not known.

A literature survey revealed that there is a limited amount of experimental heat-transfer and pressure drop data available for forced convective flow through porous wire mesh (referred to by other authors as porous media) and the majority of these data are for constant property conditions. Reference 1, which summarizes the results of the Stanford-Office of Naval Research program on compact heat-transfer surfaces, provides most of the existing data on individual wire mesh elements of different wire diameters and porosities. By using a transient test technique and constant property conditions, this program determined heat-transfer correlations for each mesh. Reference 2 revised these data and obtained a general correlation for all mesh. Similarly the isothermal pressure drop data for each mesh correlated individually with the Fanning type equation, but a general correlation for all meshes was not obtainable. Reference 3 provides the only available variable property heat-transfer and pressure drop data. The data were obtained for steady-state flow of air through an electrically heated tube bank at surface temperatures up to 1100° R.

A considerable amount of pressure drop data are available for fluid flow through packed beds (ref. 4). A comparison between wire mesh and packed beds indicates the pressure drop characteristics of both are dependent on the same basic parameters, that is, mass velocity, fluid properties, and geometrical factors. The correlations reported for packed beds are used as a basis for correlating the pressure drop data of this report.

This report presents experimental variable property pressure drop and heat-transfer correlations for helically coiled wire mesh at average surface temperatures to 5200° R. Six different meshes were tested. The wire diameter varied from 0.020 to 0.035 inch with mesh porosities between 0.640 to 0.722. The mass velocity through these mesh was varied from 0.4 to 3.1 pounds per second per square foot for hydrogen and from 4.5 to 10.2 pounds per second per square foot for nitrogen. The heat flux ranged from 0.5 to 8.3 Btu per second per square inch.

→ 22

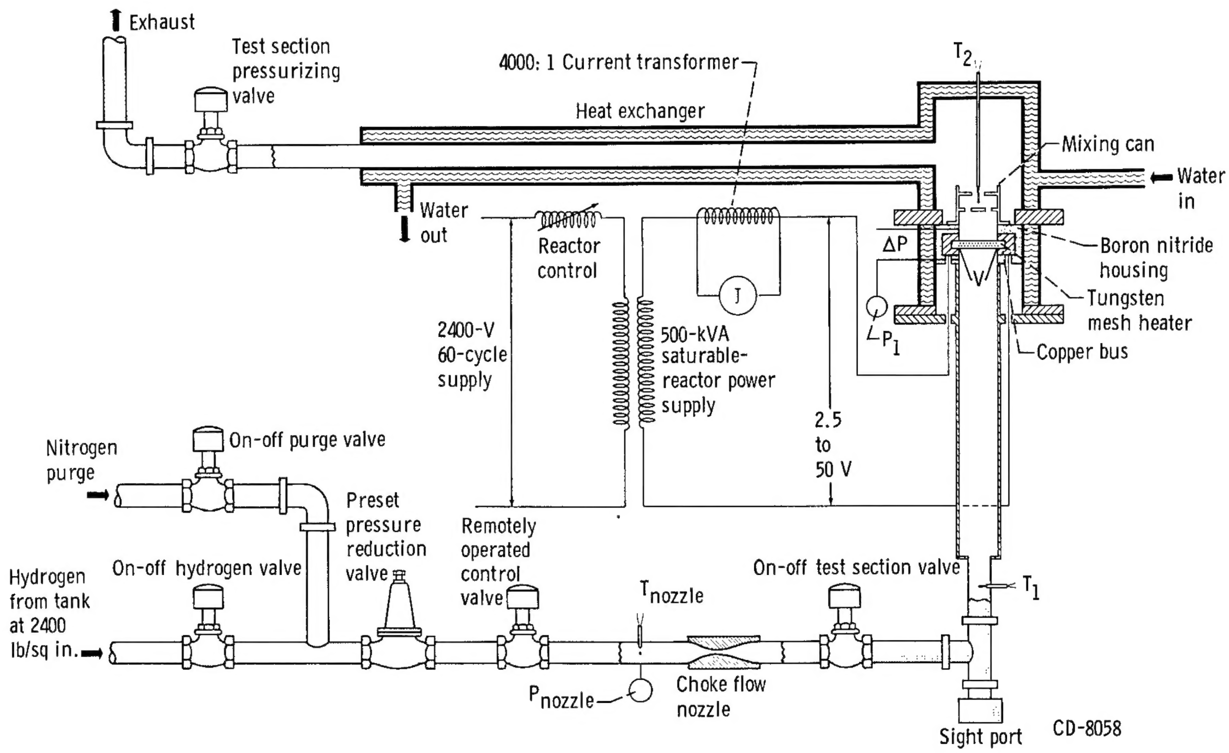

Figure 1. - Schematic diagram of test section apparatus and location of instrumentation.

APPARATUS AND PROCEDURE

A schematic diagram of the flow system, test section, power supply, instrumentation, and corresponding components associated with each, as used in this investigation, is shown in figure 1.

Flow System

As may be seen in figure 1, hydrogen or nitrogen was supplied to the flow system from a tube trailer at a maximum pressure of 2400 pounds per square inch. From the trailer the gas then flowed through a preset pressure reducer valve, a remotely operated control valve, a choked flow nozzle and an on-off valve that supplied gas directly to the test section. The gas flow was metered by means of the choked flow nozzle that assured a constant mass flow through the test section. From the test section the heated gas flowed through a two-baffle molybdenum mixing can and into a gas to water concentric tube heat exchanger where it was cooled below 1000° R before being exhausted into the atmosphere.

For safety purposes, the entire system was purged with nitrogen before hydrogen entered the system, and the controls were set for fail safe operation so if a predetermined safety permissive stops the hydrogen flow, nitrogen would automatically purge the system. In such a case, the electrical test power would also be automatically shut down.

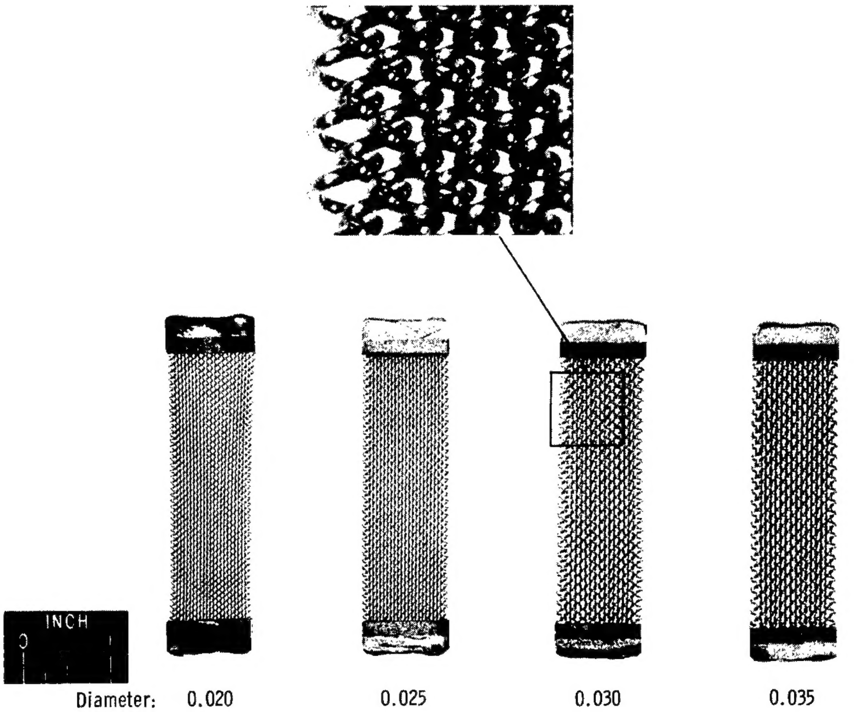

Figure 2. - Tungsten wire mesh.

TABLE I. - MESH GEOMETRIC PARAMETERS

Mesh number	1	2	3	4	5	6
Wire diameter, d, in.	0.020	0.025	0.030	0.035	0.020	0.025
Mandrel diameter, D, in.	0.060	0.060	0.080	0.080	0.060	0.060
Equivalent diameter, D_e, ft	0.00425	0.00372	0.00635	0.00642	0.00425	0.00404
Mesh size (length × width), in. × in.	3 × 1	3 × 1	3 × 1	3 × 1	3 × 3	3 × 3
Number of parallel coils, N	23	23	17	16	69	69
Coil pitch, p, in./turn	0.0666	0.0814	0.111	0.125	0.0666	0.077
Porosity, ϵ	0.722	0.640	0.717	0.685	0.722	0.660

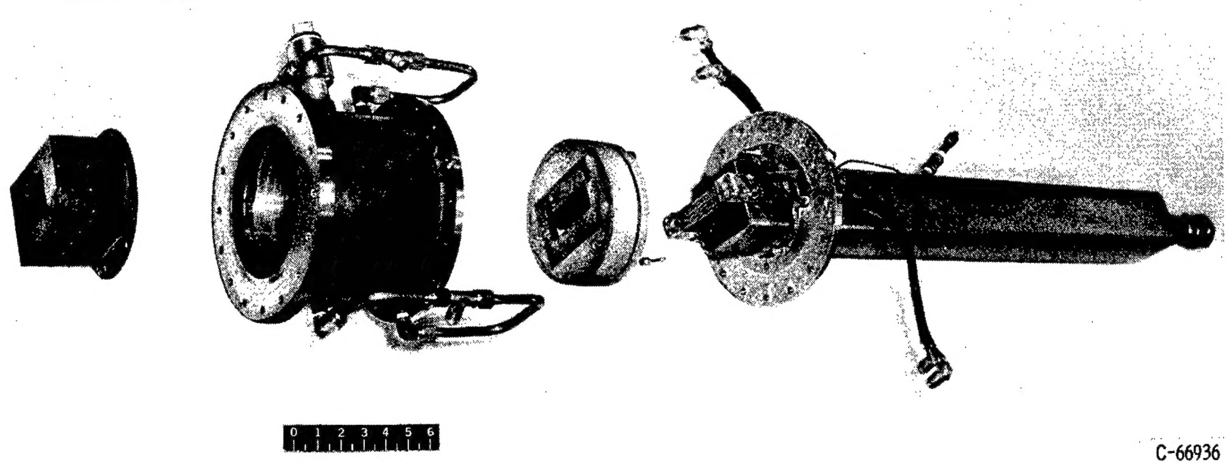

Figure 3. - Exploded view of test section assembly.

Test Section

Experiments were performed on a test section consisting of mesh formed by interwound helical coils of tungsten wire as shown in figure 2. Each end of the coils is sandwiched between two tungsten plates, approximately 0.060 inch thick, and the coils are heliarc welded at the ends of the plates to provide positive mechanical and electrical connections.

Four different 3- by 1-inch meshes were tested, each having a different wire diameter and porosity. Also tested were two 3- by 3-inch meshes, one of which has the same parameters as one of the 3- by 1-inch meshes. Table I lists the geometrical parameters associated with each mesh. The smaller 3- by 1-inch meshes were used for most of the data because they permitted investigation of higher ranges of mass velocities and heat fluxes and approximated the geometry of the final heater design.

Figure 3 shows an exploded view of the test section assembly, which consists of a 3-foot entrance transition section to straighten the gas flow prior to entry into the test section, a boron nitride housing designed to hold and electrically insulate the mesh bus connections and to minimize bypass of the gas around the mesh, a water-jacketed stainless-steel outer housing, and a molybdenum can to mix the gas prior to measuring its temperature. A rubber O-ring near the cold end of the boron nitride housing prevented leakage of the gas between the boron nitride and the stainless-steel outer support housing. No provision was made for expansion of the mesh. During initial heating, bowing occurred in the flow direction, and the mesh retained a permanent set after cooling. This set could not be changed even by reversing the mesh and heating to 5000° R at high flow rates.

Power Supply

A single phase 60-cycle 500-kilovolt-ampere saturable-reactor controlled

power supply was used to electrically heat the tungsten mesh. Output voltage was varied from 4.7 to 50 volts with a maximum current rating of 10 000 amperes. With bus losses, however, the maximum power to the test element was limited to 225 kilowatts.

Instrumentation

The location of the instrumentation is shown in figure 1. The voltage across and the current through the test section were measured. The test section voltage was taken directly across the mesh to eliminate any error caused by a voltage drop between the power supply and the test section. A true root-mean-square voltmeter was used to measure the test voltage because of the wave form produced by the saturable-reactor controlled power supply. Current was read on a precision ammeter through a 4000:1 step down current transformer. Inlet pressure to the test section was measured with a calibrated 0- to 100-pound-per-square-inch Bourdon tube gage. The pressure drop across the mesh was continuously recorded with a ±1-pound-per-square-inch temperature-compensated strain-gage bridge differential pressure transducer. Inlet temperature was measured with a type K thermocouple (designation ref. 5), and the exit temperature was measured with a platinum/platinum-13-percent-rhodium thermocouple. The exit thermocouple was placed in a baffled molybdenum mixing can to give a true mixed bulk gas temperature. Pressure and temperature measurements at the inlet to the choked flow nozzle were made. The mass flow rate was set by adjusting the nozzle inlet pressure.

METHOD OF CALCULATION

Geometrical Factors

The mesh heating elements were made of interwound helical tungsten coils. These mesh can be completely specified by five parameters: wire diameter d, mandrel diameter D, number of parallel coils N, length of mesh b, and helical coil pitch p. (All symbols are defined in the appendix.)

The geometrical parameters and corresponding equations associated with the calculation of the heat transfer, pressure drop, and mesh surface temperature for the data of this report are as follows:

The length of a single helical coil S is given by the equation

$$S = \frac{b}{p} \sqrt{\pi^2(D + d)^2 + p^2} \tag{1}$$

while the thickness of the mesh in the direction of flow is given by

$$L = D + 2d \tag{2}$$

and the total heat-transfer surface area for N number of coils is

$$A_s = \pi dSN$$

The equivalent diameter for porous media is normally defined as

$$D_e = \frac{4(\text{void volume})}{A_s} = \frac{4LA_{fl}}{A_s} \tag{4}$$

where the average flow area is given as

$$A_{fl} = \epsilon A_{ft} \tag{5}$$

The porosity is defined as the average porosity for the entire mesh volume by

$$\frac{\text{Volume of mesh - Volume of tungsten in mesh}}{\text{Volume of mesh}} = \epsilon \tag{6}$$

Average Heat-Transfer Coefficients

The average heat-transfer coefficient was computed from the experimental data by the relation

$$h = \frac{q}{A_s(T_s - T_b)} = \frac{Wc_{p,b}(T_2 - T_1)}{A_s(T_s - T_b)} \tag{7}$$

where

$$T_b = \frac{T_1 + T_2}{2} \tag{8}$$

The average surface temperature T_s of the mesh was determined from the relation between temperature and resistivity of tungsten as given in reference 6. The resistivity was calculated by

$$\zeta = \frac{V}{I}\frac{A_e}{S} \tag{9}$$

where

$$A_e = \frac{N\pi d^2}{4} \tag{10}$$

Average screen surface temperatures from the resistivity temperature relation calculated by equation (9) were verified by means of an optical pyrometer that was sighted through a port located in the inlet transition section of the test section housing. Optical pyrometer measurements indicated that the entire mesh operated within ±300° R of the same temperature over its entire frontal area.

Average Friction Pressure Drop

Static pressure taps were located in the boron nitride tunnel close to the mesh to minimize any pressure drop due to friction on the tunnel walls.

The total static pressure drop across the mesh ΔP_t is made up of three components, a combined expansion and contraction pressure drop, a momentum pressure drop, and a friction pressure drop.

Neither the expansion nor the contraction losses are experimentally separable from the friction pressure drop as in the case of tube-type flow. They are therefore included as part of the friction pressure drop.

The relation between these components is expressed by the following equation:

$$\Delta P_t = \frac{G^2}{g}\left(\frac{1}{\rho_2} - \frac{1}{\rho_1}\right) + \Delta P \tag{11}$$

where $G^2/g\left[(1/\rho_2) - (1/\rho_1)\right]$ is the momentum pressure drop and ΔP is the friction pressure drop (including expansion and contraction effects). The mean density for the friction pressure drop calculations as used in equation (11) is evaluated from the static pressures and total temperatures of the gas as follows:

$$\rho_m = \frac{1}{R}\,\frac{P_1 + P_2}{T_1 + T_2} \tag{12}$$

The difference between the total and static temperatures of the gas was never more than 1/2 percent. Total gas temperatures were therefore used in these calculations.

RESULTS AND DISCUSSION

The data obtained from this investigation are presented in table II. Differences between the total electrical heat input and the heat transferred to the gas were due to radiation and conduction losses to the water-cooled buses and jacketed housing.

Heat Transfer

Flow normal to a wire mesh heat-transfer surface is somewhat analogous to flow past a single cylinder in an infinite fluid because the flowing fluid forms a laminar boundary layer on the front portion of the cylinders. Proceeding around a cylinder, the flow accelerates and then decelerates, which causes separation of the boundary layer from the surface producing a turbulent wake behind the cylinder. The heat transferred from the upstream portion of the cylinder where the laminar boundary layer exists can be calculated from the

TABLE II. - TABULATION OF HEATED AND ISOTHERMAL DATA

Run	Mesh number	Voltage, V	Current, I, amp	Average surface temperature, T_s, °R	Gas	Inlet gas temperature, T_1, °R	Outlet gas temperature, T_2, °R	Gas flow rate, W, lb/sec	Inlet pressure, P_1, lb/sq in. gage	Total static pressure drop, ΔP_t, lb/sq in.
Heated										
1	1	28.5	1280	2283	Hydrogen	520	985	0.0199	2.40	0.159
2		39.1	1340	2875			1185	.0199	2.60	.219
3		50.1	1565	3110			1185	.0297	5.20	.395
4		39.2	1520	2585			1025	.0297	5.00	.325
5		29.5	1445	2120			885	.0297	4.70	.265
6		30.6	1560	2048			825	.0410	7.20	.194
7		43.6	1650	2638			965	.0410	7.80	.454
8		51.5	1690	2980			1070	.0410	8.10	.504
9		49.5	1640	2950			1100	.0349	6.60	.435
10		29.0	1500	2023			845	.0349	5.90	.305
11	2	15.0	1805	1618	Hydrogen	520	870	0.0199	2.60	0.259
12		29.7	1960	2680			1235		3.00	.409
13		22.9	1880	2225			1055		2.90	.339
14		37.7	2080	3152			1455		3.30	.489
15		43.8	2100	3500			1630		3.50	.539
16		49.8	2160	3800			1815		3.60	.589
17		48.4	2360	3450			1470	.0297	6.10	.835
18		39.3	2280	2980			1260		5.70	.715
19		28.6	2155	2400			1040		5.20	.555
20		19.4	2080	1800			860		4.80	.445
21		20.7	2220	1780			810	.0410	7.50	.634
22		31.8	2360	2435			985		8.20	.804
23		41.0	2470	2900			1130		8.80	.964
24		50.9	2560	3345			1310		9.40	1.124
25	3	21.9	1800	2460	Hydrogen	520	975	0.0199	2.70	0.169
26		31.0	1900	3153			1200		2.90	.229
27		41.8	2000	3870			1470		3.10	.269
28		41.0	2165	3570			1235	.0297	5.40	.400
29		45.8	2205	3850			1320		5.60	.425
30		31.1	2140	2950			1040		5.10	.325
31		19.7	1920	2120			815		4.60	.225
32		31.2	2205	2790			925	.0410	7.80	.434
33		40.0	2300	3330			1060		8.20	.514
34		45.5	2360	3610			1150		8.50	.564
35		17.2	1960	1865			750	.0349	5.60	.245
36		28.5	2110	2695			925		6.20	.355
37		39.5	2220	3395			1110		6.70	.455
38		45.0	2280	3700			1200		7.00	.495
39		20.0	1780	2300			925	.0199	2.60	.149
40		41.2	2000	3820			1455	.0199	3.10	.269
41	4	23.6	2170	2900	Hydrogen	520	1160	0.0199	2.80	0.239
42		39.0	2420	4020			1655		3.30	.369
43		44.3	2520	4338			1845		3.50	.409
44		42.4	2680	3963			1445	.0297	5.90	.575
45		36.2	2570	3585			1290		5.60	.515
46		23.1	2390	2638			985		5.00	.375
47		23.0	2550	2490			885	.0411	7.60	.494
48		35.0	2720	3345			1110		8.40	.654
49		44.3	2860	3900			1280		9.00	.764
50		23.2	2470	2570			925	.0349	6.20	.435
51		34.5	2640	3395			1160		7.00	.585
52		44.5	2780	4020			1370		7.50	.685
53		49.0	2860	4250			1480		7.70	.735
54		13.4	2000	1925			845	.0199	2.50	.159
55		44.2	2520	4338			1785	.0199	3.50	.409
56		49.3	2880	4213			1520	.0349	7.70	.715
57		49.3	2890	4213			1520		7.80	.715
58		49.3	2890	4213			1530		7.80	.705

TABLE II. - Continued. TABULATION OF HEATED AND ISOTHERMAL DATA

Run	Mesh number	Voltage, V	Current, I, amp	Average surface temperature, T_s, ^oR	Gas	Inlet gas temperature, T_1, ^oR	Outlet gas temperature, T_2, ^oR	Gas flow rate, W, lb/sec	Inlet pressure, P_1, lb/sq in. gage	Total static pressure drop, ΔP_t, lb/sq in.
59	4	22.4	1280	4325	Nitrogen	515	1270	0.170	----	----
60		14.8	1094	3500			1070	.0866	----	----
61		19.6	1160	4200			1255	.0866	----	----
62		13.6	1010	3475			1125	.0665	----	----
63		16.6	1082	3885			1255	.0665	----	----
64		9.5	1121	2365			785	.1270	----	----
65		24.0	1320	4485			1200	.1270	----	----
66		26.9	1396	4700			1215	.1460	----	----
67		22.8	1320	4285			1115		----	----
68		16.1	1280	3280			945		----	----
69		11.8	1185	2710			820		----	----
70		30.0	1420	5065			1280		----	----
71		32.0	1460	5213			1335		----	----
72	3	16.6	1000	3203	Nitrogen	515	865	0.1460	----	------
73		23.3	1080	2975			1005		----	------
74		31.2	1180	4725			1195		----	------
75		12.6	960	2625			810	.127	----	------
76		18.0	1000	3420			945		----	------
77		23.1	1044	4075			1085		----	------
78		28.0	1100	4588			1185		----	------
79		10.9	920	2400			790	.1070	----	------
80		17.9	960	3515			990		----	------
81		24.5	1040	4270			1180		----	------
82		11.1	880	2545			860	.0866	----	------
83		14.2	880	3140			955		----	------
84		20.0	920	4010			1135		----	------
85		24.9	1000	4485			1290		----	------
86		12.4	840	2900			975	.0665	----	------
87		16.6	840	3700			1130		----	------
88		23.0	940	4430			1365		----	------
89		29.6	1000	5173			1630		----	------
90	5	41.0	3380	3420	Hydrogen	510	1880	0.0223	----	------
91		46.5	3480	3700			2090		----	------
92		49.3	3548	3835			2223		----	------
93		37.0	3140	3395			2100	.0178	----	------
94		42.4	3240	3650			2257		----	------
95		46.0	3340	3820			2400		----	------
96		8.6	2760	1085		535	685	.0389	----	------
97		17.2	3140	1765			885		----	------
98		26.5	3320	2400			1130		----	------
99		47.0	3780	3488			1660		----	------
100		16.8	3040	1780			915	.0339	----	------
101		26.5	3240	2456			1200		----	------
102		32.0	3380	2777			1325		----	------
103		13.8	2760	1630			865	.0286	----	------
104		21.5	2960	2225			1095		----	------
105	6	4.5	3260	920	Hydrogen	560	645	0.0389	----	------
106		7.8	4040	1219			750		----	------
107		11.1	4440	1522			865		----	------
108		13.7	4560	1780			955		----	------
109		28.2	5060	3005			1480		----	------
110		7.3	4160	1130		540	740	.0391	----	------
111		11.2	4520	1510			865		----	------
112		19.2	4800	2265			1130		----	------
113		25.9	5080	2790			1405		----	------
114		5.7	3780	992			695	.0339	----	------
115		11.8	4320	1645			920	.0339	----	------

TABLE II. - Concluded. TABULATION OF HEATED AND ISOTHERMAL DATA

Run	Mesh number	Voltage, V	Current, I, amp	Average surface temperature, T_s, $^{\circ}R$	Gas	Inlet gas temperature, T_1, $^{\circ}R$	Outlet gas temperature, T_2, $^{\circ}R$	Gas flow rate, W, lb/sec	Inlet pressure, P_1, lb/sq in. gage	Total static pressure drop, ΔP_t, lb/sq in.
Isothermal										
116	1	----	----	----	Hydrogen	520	520	0.0124	1.30	0.0210
117		----	----	----				.0178	2.00	.0415
118		----	----	----				.0232	2.70	.0550
119		----	----	----				.0285	3.60	.0770
120		----	----	----				.0338	4.60	.0875
121		----	----	----				.0391	5.60	.1070
122	2	----	----	----	Hydrogen	520	520	0.0178	2.00	0.0915
123		----	----	----				.0232	2.70	.1450
124		----	----	----				.0285	3.70	.1970
125		----	----	----				.0338	4.80	.2570
126		----	----	----				.0391	6.00	.3170
127	3	----	----	----	Hydrogen	520	520	0.0178	2.00	0.0415
128		----	----	----				.0232	2.70	.0550
129		----	----	----				.0285	3.50	.0770
130		----	----	----				.0338	4.60	.0975
131		----	----	----				.0391	5.80	.1170
132	4	----	----	----	Hydrogen	520	520	0.0178	2.00	0.0515
133		----	----	----				.0232	2.70	.0850
134		----	----	----				.0285	3.60	.1170
135		----	----	----				.0338	4.80	.1470
136		----	----	----				.0391	5.90	.1870
137	1	----	----	----	Nitrogen	520	520	0.0261	0.70	0.0080
138		----	----	----				.0465	1.10	.0170
139		----	----	----				.0666	1.90	.0310
140		----	----	----				.0866	2.50	.0500
141		----	----	----				.1070	3.50	.0670
142		----	----	----				.1270	4.50	.0870
143		----	----	----				.1460	5.60	.1040
144	2	----	----	----	Nitrogen	520	520	0.0465	1.20	0.0460
145		----	----	----				.0666	1.90	.0850
146		----	----	----				.0866	2.70	.1350
147		----	----	----				.1070	3.60	.1870
148		----	----	----				.1270	4.65	.2470
149		----	----	----				.1460	5.90	.3070
150	3	----	----	----	Nitrogen	520	520	0.0465	1.20	0.0210
151		----	----	----				.0866	2.60	.0550
152		----	----	----				.1070	3.50	.0770
153		----	----	----				.1270	4.50	.0925
154		----	----	----				.1460	5.60	.1170
155	4	----	----	----	Nitrogen	520	520	0.0261	0.70	0.0090
156		----	----	----				.0465	1.20	.0230
157		----	----	----				.0666	1.90	.0410
158		----	----	----				.0866	2.60	.0700
159		----	----	----				.1070	3.50	.0990
160		----	----	----				.1270	4.60	.1280
161		----	----	----				.1460	5.70	.1620

analytical relation that Nusselt number is proportional to the square root of the Reynolds number ($Nu \propto \sqrt{Re}$ (ref. 7)). However, the downstream portion of the cylinder where the flow separates defies analysis, and therefore experimental data must be used to empirically predict the total heat transfer from such a surface. The presence of adjacent cylinders affects the boundary layer thickness, velocity distribution, and also the nature of the turbulent wake. If the cylinders are interwoven into a mesh, the effective heat-transfer area is less than the total mesh surface area due to wire overlap. The absence of a general correlation for flow through porous media indicates the difficulty in defining the geometrical factors that influence both the heat-transfer and pressure drop characteristics of the system.

The usual dimensionless groups were used to correlate the heat-transfer data by the relation

$$Nu = F\left[(Re)(Pr)\right] \tag{13}$$

Variable fluid properties and mesh geometry significantly affected the magnitude of these groups. The fluid properties were evaluated at the average bulk, film, and surface temperatures to determine which reference temperature best represented the variable property effects. The changing geometry that the fluid encountered in passing through the mesh was represented by the porosity factor included in the definitions of equivalent diameter D_e and flow area A_{fl} as defined in the section METHOD OF CALCULATION.

Figures 4(a), (b), and (c) show the correlation of the heat-transfer data on a bulk, film, and surface temperature basis, respectively. Evaluation of the equilibrium fluid properties at the surface temperature produced the best correlation. The physical properties for hydrogen were taken from reference 8 and for nitrogen from reference 9. The maximum deviation of the data from the correlating equation was ±14 percent for the surface temperature correlation as compared to ±20 percent and ±29 percent for the film and bulk temperature correlations, respectively.

The equation

$$Nu_s = 0.462\, Re_s^{0.53} Pr_s^{0.40} \tag{14}$$

represents the heat-transfer correlation of six helically coiled wire meshes for the following range of properties and conditions:

(1) Porosity of 64 to 72.2 percent

(2) Wire diameter of 0.020 to 0.035 inch

(3) Surface temperature of 1400° to 5200° R

(4) Outlet gas temperature of 600° to 2400° R

(5) Mass velocity for hydrogen of 0.4 to 3.1 pounds per second per square foot and for nitrogen of 4.5 to 10.2 pounds per second per square foot

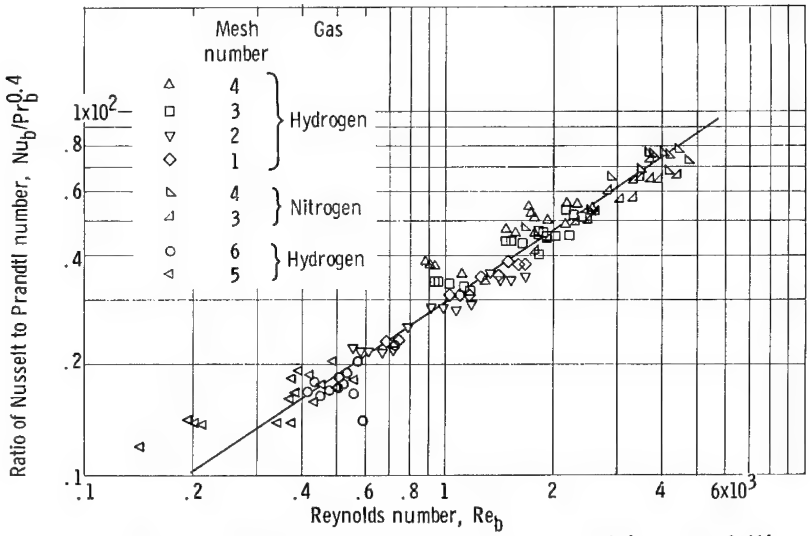

(a) Fluid properties evaluated at bulk temperature. $Nu_b/Pr_b^{0.4} = 0.303\ Re_b^{0.664}$.

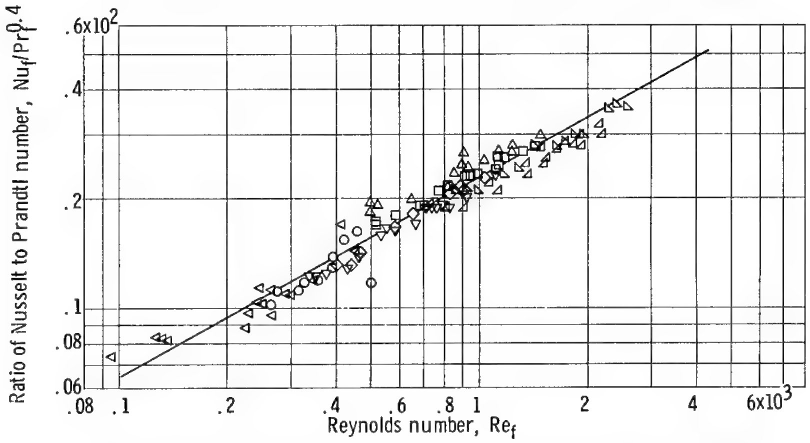

(b) Fluid properties evaluated at film temperature. $Nu_f/Pr_f^{0.4} = 0.50\ Re_f^{0.552}$.

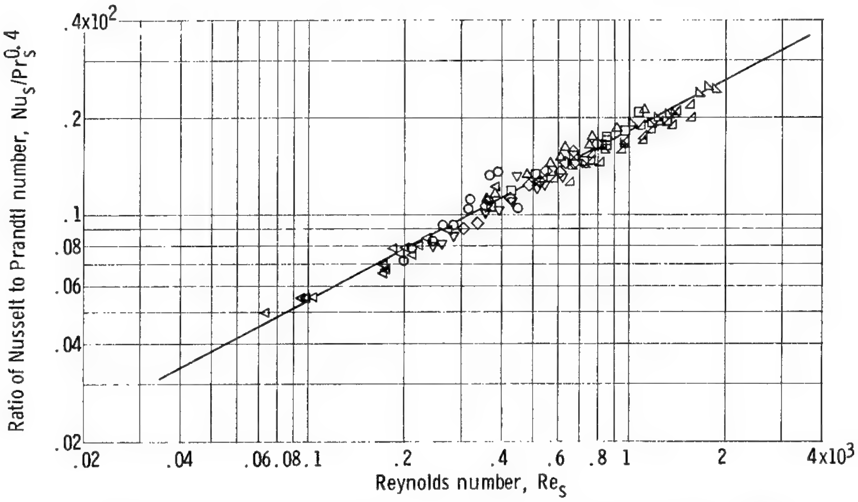

(c) Fluid properties evaluated at surface temperature. $Nu_s/Pr_s^{0.4} = 0.462\ Re_s^{0.53}$.

Figure 4. - Correlation of heat-transfer data using equilibrium fluid properties evaluated at bulk, film, and surface temperatures.

(6) Heat flux of 0.5 to 8.3 Btu per second per square inch

(7) Pressure level of 1 atmosphere

Practically all of the heat-transfer data presented in the literature for a mesh-type configuration were obtained at low-temperature constant property conditions. The majority of these data were obtained by the Stanford-ONR program on compact heat-transfer surfaces (ref. 1). These investigators studied several woven wire mesh heat-transfer surfaces of different wire diameters and porosities. They were able to determine the heat-transfer characteristics for each mesh but did not present a general correlation for all of the meshes. These data were obtained by a transient test technique whereby the mesh test element was heated to a uniform temperature either in a furnace or by a stream of hot gas and then immediately subjected to a lower temperature gas stream. The time-temperature history of the gas leaving the test element provides the information necessary to calculate the heat-transfer characteristics of the system.

In reference 2, the Stanford-ONR data were revised by substituting the wire diameter d for the equivalent diameter D_e and applying a correction factor for that part of the surface area where the wires overlap and reduce the heat-transfer surface. The revised Stanford-ONR data for six meshes resulted in one general correlation.

Reference 3 studied air flow through electrically heated wire tube banks for variable property conditions. Their heat-transfer results based on the film temperature agreed fairly well with the single wire equation of reference 10.

Figure 5 compares this report's correlation with the correlations of references 2, 3, and 10. The Prandtl number was excluded because it was similar for all investigations. A direct comparison was not possible because of the following differences:

(1) The fluid velocity for all correlations except reference 10 was based on average flow area throughout the mesh as defined by frontal area times porosity. For the single wire data of reference 10, the frontal velocity was used to characterize the flow.

(2) References 2, 3, and 10 used wire diameter as the characteristic dimension, whereas the equivalent diameter was used for the data of this investigation.

(3) The data of other investigators were obtained at low temperatures under relatively constant property conditions as compared to the variable property data of this investigation.

(4) The total surface area was used to evaluate the heat-transfer coefficient for the data of this investigation because it was not possible to accurately define the amount of wire overlap as in reference 2.

The good agreement of the single-wire correlation of reference 10 and the

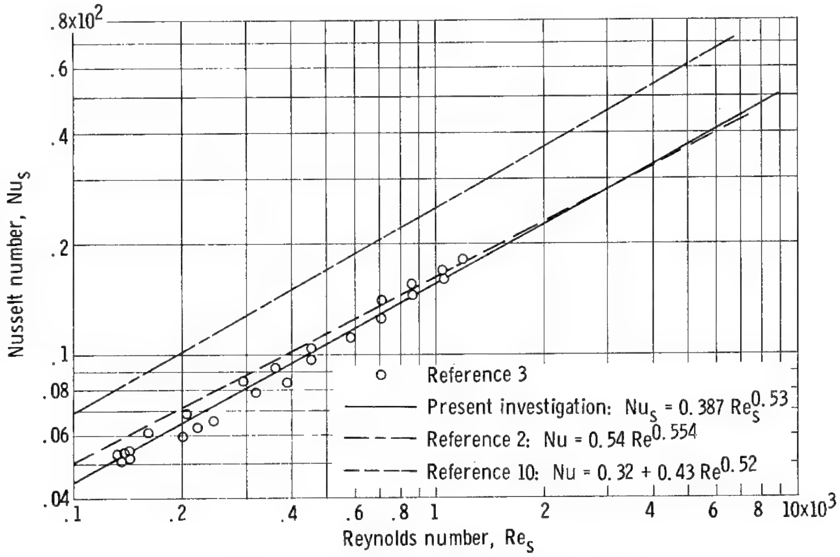

Figure 5. - Comparison of other correlations and data with correlation of this investigation.

multiwire tube bank data of reference 3 indicates that the effect of adjacent wires on heat transfer is not significant if the wires do not engage. The differences in the mesh correlations of reference 2 and this report are indicative of the geometry differences between a woven wire mesh and an interwound coil mesh.

The significance of figure 5 lies in the fact that all of the correlations have similar slopes approximating 0.5, which indicates that the forced convective heat transfer for any mesh is primarily a function of the laminar boundary layer conditions on the upstream portion of the mesh surface as defined analytically by $Nu \propto C\sqrt{Re}$ (ref. 7). Deviations from this square-root function indicate the effect of turbulence created by the different types of mesh geometries. Differences in the coefficient C of the various correlating equations are due to the geometrical factors such as equivalent diameter, flow area, and actual heat-transfer surface area. These factors, which are different for each mesh, preclude a universal heat-transfer correlation for all meshes.

Pressure Drop

The friction pressure drop, as previously mentioned, is made up of two inseparable components (1) a friction component, associated with the surface resistance of the wire mesh and (2) an expansion and contraction component, associated with the area changes the fluid encounters in passing through the mesh. Some investigators (refs. 1, 11, 12, and 13) have used the conventional Fanning equation, which is generally used for fully developed flow through tubes, to correlate pressure drop data for mesh geometries. This has resulted in individual correlations for each mesh. In comparing wire mesh with packed beds it became apparent that pressure drop in both is dependent upon the same parameters, namely, flow rate, viscosity and density of fluid, porosity, packing, size, shape, and surface of the solid. This indicated that a pressure drop correlation similar to that used for packed beds might also be applicable to wire mesh. Following is a more detailed discussion on the methods used for correlating the friction pressure drop data.

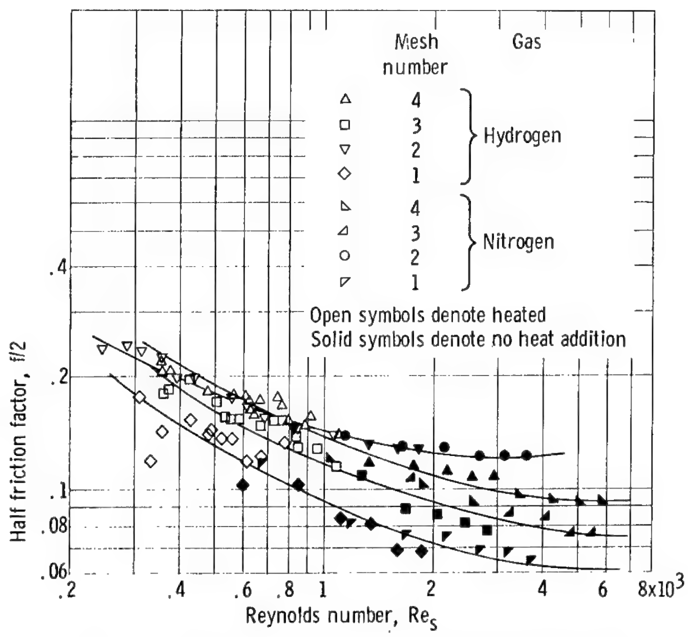

Figure 6. - Correlation of average half friction factor with Reynolds number using conventional Fanning type correlation.

The conventional Fanning equation used to calculate the friction-factor data is expressed by

$$\frac{f}{2} = \frac{\Delta P g \rho_m D_e}{4LG^2} \qquad (15)$$

This equation was used by investigators in references 1, 11, 12, and 13. With the exception of the data of reference 3, pressure drop data of the other investigations has been isothermal. Since this report includes pressure drop data with and without heat addition for hydrogen and without heat addition for nitrogen, a variable property correlation was used. Figure 6 shows $f/2$ plotted against Reynolds number for the heated and isothermal data for each of the four 3- by 1-inch meshes tested. The mean fluid density was evaluated on a bulk temperature basis (eq. (12)) and the viscosity on a surface temperature basis. Other combinations of evaluating fluid density and viscosity for the heated data on bulk, film, and surface temperatures were attempted but resulted in more scatter. A comparison of the variable property plots of figure 6 with similar isothermal plots of references 12 and 13 indicates the following similarities exist for meshes of different geometries but within approximately the same porosity range:

(1) The friction factors are of the same order of magnitude

(2) The slopes of the curves are similar for the same Reynolds number

(3) A gradual change of slopes occurs between different flow regimes with changing Reynolds number

(4) The curves of the same type mesh sometimes cross

The conventional Fanning type equation although providing a means of evaluating friction factors of individual mesh is limited in use to mesh for which pressure drop data has already been experimentally determined. This equation provides the only means of comparing the data contained herein with that of other investigators. The complexity of the flow through the mesh precludes the fact that a general correlation could be obtained by use of the conventional Fanning equation. This led to a method of correlation that can be easily converted to a modified Fanning type equation, discussed later, and which has been successfully used by previous investigators for packed bed geometries.

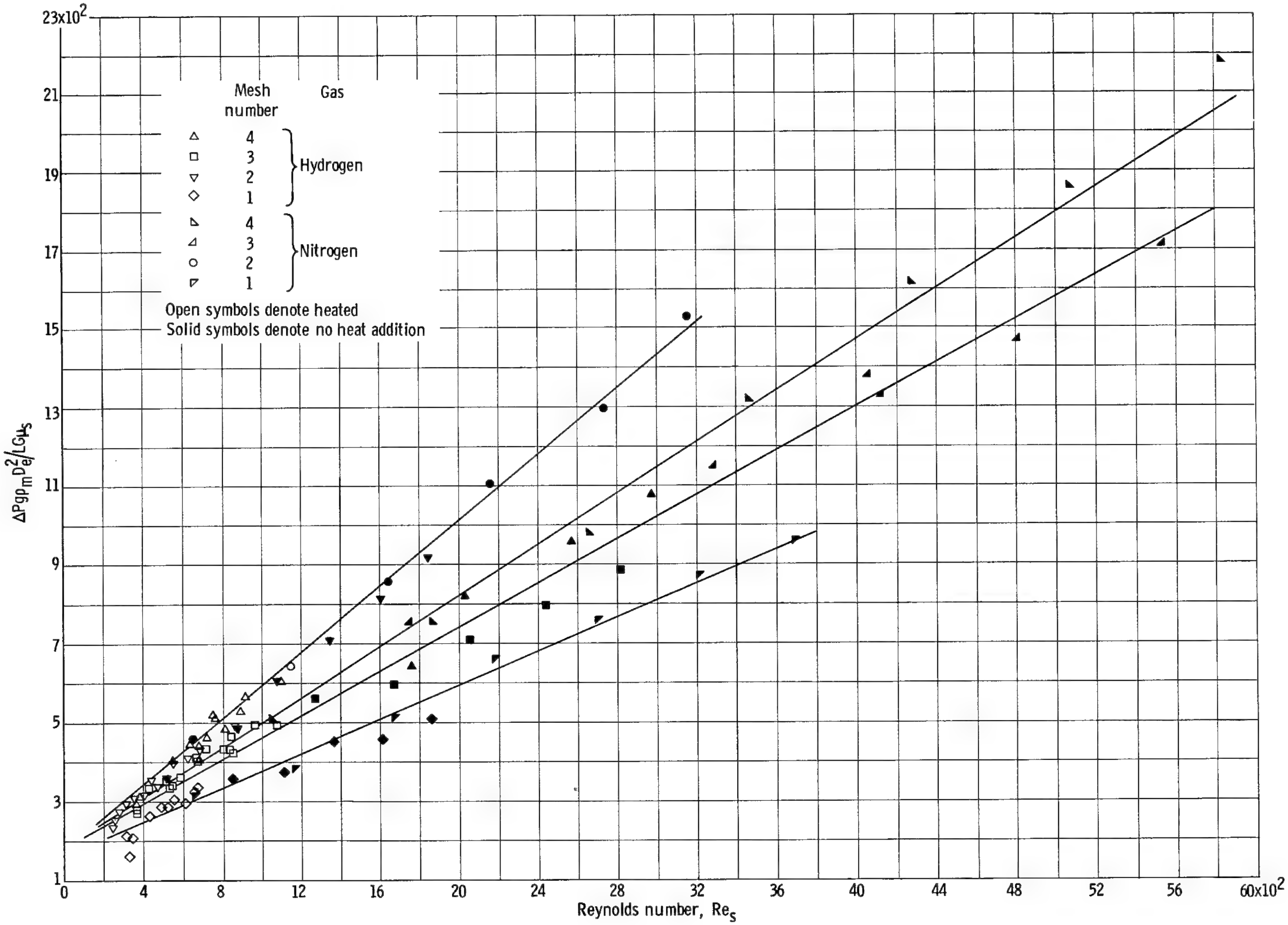

Figure 7. - Pressure drop correlation based on method used in reference 14.

Reference 4 discusses the factors to be considered in correlating parameters that determine energy losses in packed beds. It further gives a good survey of references applicable to packed bed pressure measurements.

Reference 14 represents the pressure gradient by an equation of the form

$$\frac{\Delta P}{\Delta L} = \frac{\mu^2}{g\rho D_e^3} F(Re) \tag{16}$$

where, for laminar flow, $\Delta P/\Delta L$ is proportional to the Reynolds number Re and, for turbulent flow, $\Delta P/\Delta L$ is proportional to the square of the Reynolds number Re^2. In a porous mesh, pressure losses are due to both viscous shear and inertia effects associated with laminar and turbulent flow, respectively. The pressure gradient according to reference 14 can therefore be represented by the sum of the effects of both regimes weighted by the two geometry factors α and β; that is,

$$\frac{\Delta P}{\Delta L} = \frac{\mu^2}{g\rho_m D_e^3} (\alpha\ Re + \beta\ Re^2) \tag{17}$$

Dividing both sides of equation (17) by $Re\ \mu^2/g\rho_m D_e^3$ yields

$$\frac{\Delta P g\rho_m D_e^2}{\Delta L G\mu} = \alpha + \beta\ Re \tag{18}$$

Since α and β are constants dependent upon screen geometry, equation (18) is in the form of a straight line $(y = mx + b')$. The advantage of this form of friction factor $\left(f = \Delta P g\rho_m D_e^2/\Delta L G\mu\right)$ is that it is a linear function of the Reynolds number and therefore plots as a straight line on an arithmetic scale. A plot of the isothermal and heated data as shown in figure 7 indicates a straight line can be drawn through the data of each of the four meshes as predicted by equation (18). Since the mesh data plot in the order of porosity, the addition of a porosity factor to the left side of equation (18) was attempted. This should provide a means of plotting the data of all the meshes on a single curve. The best factor was found to be a porosity cube term (ϵ^3). This was determined to be the optimum value, since larger powers of porosity although bringing the isothermal data closer, caused the heated data to re-spread so it was no longer in the order of porosity. Hence,

$$\frac{\Delta P g\rho_m D_e^2 \epsilon^3}{\Delta L G\mu_s} = \alpha + \beta\ Re_s \tag{19}$$

where α and β are 48 and 0.1095, respectively, for the data of this investigation.

Figure 8 shows a plot of $\Delta P g\rho_m D_e^2 \epsilon^3/\Delta L G\mu_s$ as a function of Reynolds number ranging from 200 to 6000. This provides a straight line correlation for

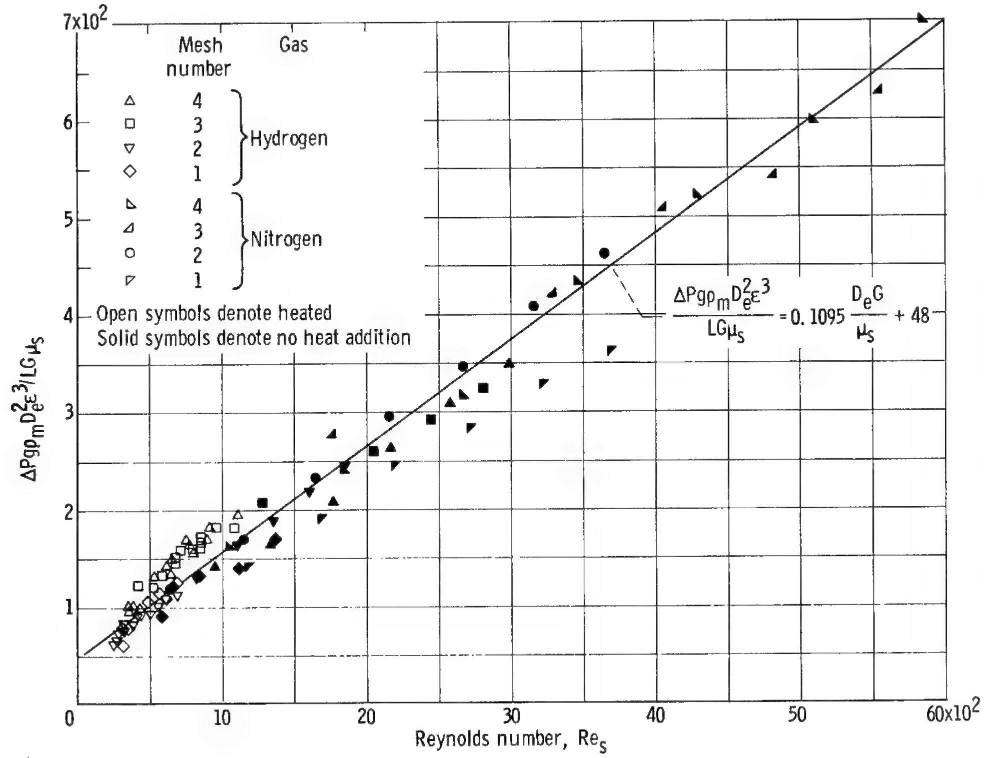

Figure 8. - Pressure drop correlation obtained by modifying method used in reference 14 by porosity cube term.

the data of all the meshes for both heated and isothermal data that has a spread of ±25 percent. It should be noted that the viscosity of the fluid is evaluated at the mesh surface temperature and the density as defined by equation (12) is evaluated at the bulk temperature. Here again, as with the conventional Fanning type correlation, the heated data was in best agreement with the isothermal data when the fluid properties were evaluated at these temperatures.

It should be noted that division of both sides of equation (19) by Reynolds number transforms this equation into a modified Fanning equation

$$\frac{\Delta P g \rho D_e \epsilon^3}{\Delta L G^2} = \frac{\alpha}{Re} + \beta = f' \tag{20}$$

where α/Re is the dominating term in the laminar flow regime and β is the dominating term in the turbulent flow regime and indicates the friction factor approaches a constant for turbulent flow. This is clearly shown in figure 6 where in the turbulent region the friction factors for each mesh approach a constant value.

An equation of the form of equation (20) could have initially been used to obtain a correlation; however, a plot of $\Delta P g \rho_m D_e / \Delta L G^2$ against Re for each mesh does not plot as a straight line and therefore increases the diffi-

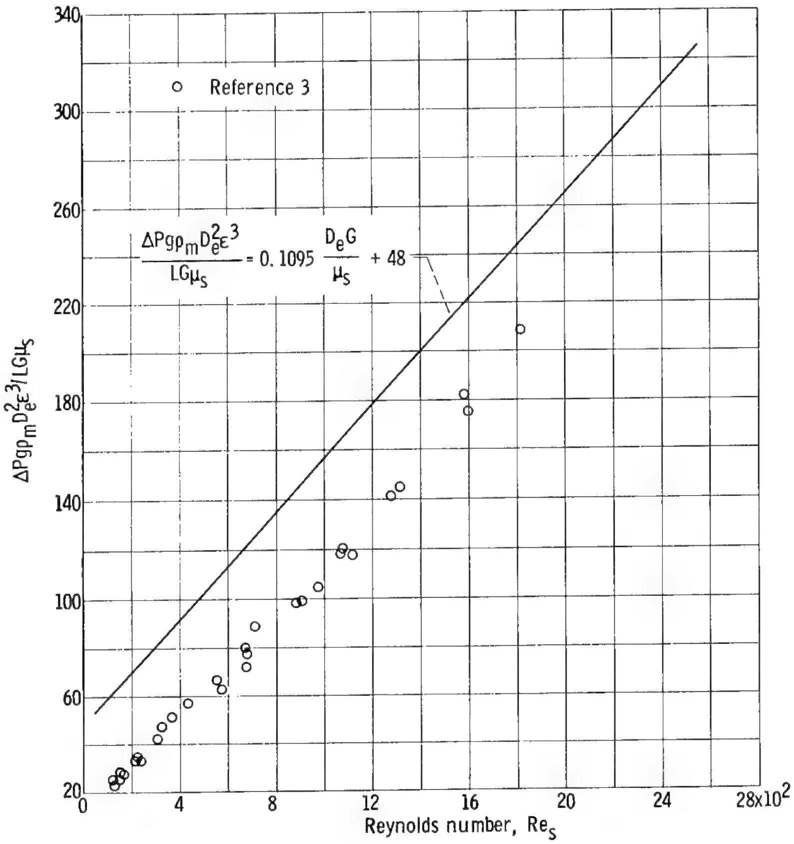

Figure 9. - Comparison of present correlating line with data of reference 3.

culty in obtaining a correlation. Therefore, the approach previously discussed was used.

Figure 9 shows the data of reference 3 for flow of air through banks of vertical rods using the correlation of this report (eq. (19)). This indicates that a similar correlation might be obtained for different types of mesh. Due to geometry differences a single correlation for all mesh would not be expected. However, if enough data on different types of mesh were available, geometry correction factors could probably be found that would enable a universal correlation to be obtained.

Effect of Screen Bypass

The correlation of Nusselt number against Reynolds number as discussed in the section Heat Transfer has been obtained with the mesh fitting into the duct cross-sectional area such that a gap of only 1/64 of an inch (about 3 percent bypass) exists along each 3-inch side of the mesh. Experimental data with hydrogen as the coolant were obtained on one mesh heater of 0.030-inch-diameter wire with a bypass area of 25 percent.

By assuming that all the heat generated in the mesh is transferred to the

gas passing through the mesh, a heat balance can be made on a mesh with bypass as follows:

$$q = W_M c_{p,b}(T_2' - T_1) \tag{21}$$

The amount of heat transferred to the gas can be represented by the heat-transfer equation

$$q = hA_s(T_s - T_b') \tag{22}$$

where

$$T_b' = \frac{T_2' + T_1}{2} \tag{23}$$

for h, the heat-transfer coefficient, the mesh correlation can be substituted as

$$h = 0.462 \frac{k_s}{D_e}\left(\frac{W_M D_e}{A_{f1}\mu_s}\right)^{0.53}\left(\frac{c_p\mu}{k}\right)_s^{0.40} \tag{24}$$

By combining equations (21) to (24), the following equation can be written for q:

$$q = \frac{0.462\left(\frac{c_p\mu}{k}\right)_s^{0.4} \frac{k_s}{D_e}\left(\frac{W_M D_e}{A_{f1}\mu_s}\right)^{0.53} A_s(T_s - T_1)}{1 + 0.462\left(\frac{c_p\mu}{k}\right)_s^{0.4} \frac{k_s}{D_e}\left(\frac{W_M D_e}{A_{f1}\mu_s}\right)^{0.53} \frac{A_s}{2W_M c_{p,b}}} \tag{25}$$

where k_s and μ_s for hydrogen can be represented as approximate functions of T_s by the following relations:

$$k_s = 1.8\times10^{-7}\ T_s^{0.8} \quad \text{for} \quad 500^\circ\ R > T_s < 3500^\circ\ R \tag{26}$$

$$\mu_s = 9.1\times10^{-8}\ T_s^{0.67} \quad \text{for} \quad 500^\circ\ R > T_s < 5000^\circ\ R \tag{27}$$

For an experimental run the following data were taken W, T_s, q, T_1, T_2, and ΔP_t. Hence all the parameters in equation (25) are known except W_M, which is then solved for. However, as a means of checking the value of W_M determined from equation (25), the total static pressure drop for the mesh was calculated with equations (11) and (19), where G is based on the calculated value of W_M flowing through the mesh. The value of ΔP_t calculated from equations (11) and (19) is then compared to the experimental ΔP_t across the mesh and the bypass. The two values of ΔP_t, measured and calculated, checked within ±25 percent, which was within the range of data scatter. For the range

of conditions run with a 25 percent bypass area, as much as 65 percent of the flow goes through the bypass region.

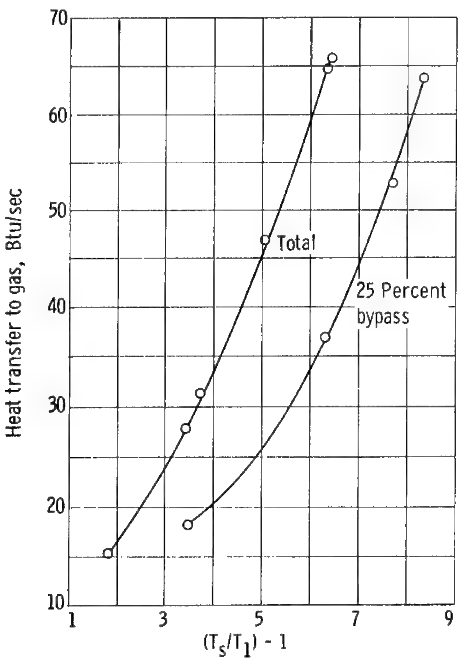

Figure 10. - Comparison of heat transfer to gas with and without bypass from experimental data. Gas flow rate, 0.0199 pound per second; inlet gas temperature, 520° R; gas, hydrogen.

To illustrate the difficulty encountered with bypass, figure 10 compares a set of experimental curves for a constant mass flow of hydrogen with and without bypass. For greater heat-transfer efficiency, a heating element should be operated near its maximum temperature. From figure 10, it is evident that to transfer a given quantity of heat with bypass a much higher surface temperature is required or for a given surface temperature much less heat is transferred. This could cause heater burnout if a mesh heater were designed without consideration of flow bypass. In order to design a heater where the bypass area is no longer insignificant (≈3 percent or more), experimental bypass flow coefficients are required in addition to the heat-transfer and pressure drop correlations.

SUMMARY OF RESULTS

Heat transfer and friction pressure drop data at 1 atmosphere were obtained for forced convection of hydrogen and nitrogen through tungsten wire mesh electrically heated to surface temperatures up to 5200° R. Outlet gas temperatures as high as 2400° R and Reynolds numbers from 200 to 6000 with fluid properties evaluated at surface temperatures were obtained. The effect of flow bypass, resulting from a mesh heater not filling a flow passage, was investigated for a bypass area of 25 percent. The following results were obtained for the mesh tested in this investigation:

1. A variable property heat-transfer correlation for helically coiled wire mesh operating at surface temperatures up to 5200° R has been obtained based on mesh geometry with fluid properties evaluated at the surface temperature.

2. A pressure drop correlation for both isothermal and heated data has been obtained based on mesh geometry with fluid properties evaluated at the surface temperature.

3. Comparison of experimental data with that of other investigators indicates a universal correlation for all types of wire mesh was not obtained because of the difficulty in evaluating the equivalent diameter, surface area, and flow area that determine the heat-transfer, pressure drop, and fluid flow parameters.

4. Flow bypassing the mesh heater element can cause serious design problems. Experimental data in addition to the heat-transfer and pressure drop correlations are required to design a heater with bypass.

Lewis Research Center,
National Aeronautics and Space Administration,
Cleveland, Ohio, April 15, 1965.

APPENDIX - SYMBOLS

A_e	current flow cross-sectional area, sq ft
A_{fl}	flow area, sq ft
A_{ft}	frontal area, sq ft
A_s	surface area, sq ft
b	length of mesh, ft (except where otherwise noted)
C	constant
c_p	specific heat of gas at constant pressure, Btu/(lb)(^{o}R)
D	mandrel diameter, ft (except where otherwise noted)
D_e	equivalent diameter, ft; four times void volume/surface area
d	wire diameter, ft (except where otherwise noted)
F	function
f	average conventional friction factor
f'	average modified friction factor
G	mass velocity through mesh, lb/(sec)(sq ft)
g	acceleration due to gravity, 32.2 ft/sec^2
h	average heat-transfer coefficient, Btu/(sec)(sq ft)(^{o}R)
I	current, amps
k	thermal conductivity of gas, Btu/(ft)(sec)(^{o}R)
L	thickness of mesh in direction of flow (characteristic length), ft
N	number of parallel coils
Nu	Nusselt number, hD_e/k
P	pressure, lb/sq ft
P_1	inlet static pressure, lb/sq ft
P_2	outlet static pressure, lb/sq ft
ΔP	friction pressure drop, lb/sq ft

ΔP_t total static pressure drop, lb/sq ft

Pr Prandtl number, $c_p\mu/k$

p coil pitch, ft/turn

q rate of heat transfer to gas, Btu/sec

R gas constant, (ft)(lb)/(lb)($^{\circ}$R)

Re Reynolds number, D_eG/μ

S total wire length of helical coil, ft

T temperature, $^{\circ}$R

T_b average bulk temperature, $(T_1 + T_2)/2$, $^{\circ}$R

T_b' average bulk temperature of unmixed gas passing through screen, $T_1 + T_2'/2$, $^{\circ}$R

T_s average surface temperature, $^{\circ}$R

T_1 inlet gas temperature, $^{\circ}$R

T_2 outlet gas temperature, $^{\circ}$R

T_2' outlet temperature of unmixed gas passing through screen, $^{\circ}$R

V voltage

W gas flow rate, lb/sec

W_M gas flow rate through mesh, lb/sec

α experimental screen geometry factor (viscous flow)

β experimental screen geometry factor (turbulent flow)

ϵ screen porosity

ζ resistivity of tungsten, ohm-ft

μ absolute viscosity of gas, lb/(sec)(ft)

ρ_m mean gas density, $(P_1 + P_2)/R(T_1 + T_2)$, lb/cu ft

ρ_1 inlet gas density, lb/cu ft

ρ_2 outlet gas density, lb/cu ft

Subscripts:

b bulk

f film

s surface

REFERENCES

1. Kays, W. M.; and London, A. L.: Compact Heat Exchangers. The National Press, 1955.

2. Lapides, M. E.; and Lawyer, J. E.: Summary of Analysis of Heat Transfer and Pressure Drop Information and Estimates Applicable to AC-1 Fuel Elements. General Electric Co., Feb. 5, 1953.

3. Gedeon, Louis; and Grele, Milton D.: Forced-Convection Heat-Transfer and Pressure-Drop Characteristics of a Closely Spaced Wire Matrix. NACA RM E54D12, 1954.

4. Ergun, Sabri: Fluid Flow Through Packed Columns. Chem. Eng. Prog., vol. 48, no. 2, Feb. 1952, pp. 89-94.

5. Anon.: Thermocouples and Thermocouple Extension Wires. Rev. Composite of RP1.9-RP1.7, Instr. Soc. Am., July 1959.

6. Anon.: Temperature, It's Measurement and Control in Science and Industry. American Institute of Physics. Reinhold Pub. Corp., 1941, p. 1318.

7. Eckert, E. R. G.: Introduction to the Transfer of Heat and Mass. McGraw-Hill Book Co., Inc., 1950, p. 95.

8. Grier, Norman T.: Calculation of Transport Properties and Heat-Transfer Parameters of Dissociating Hydrogen. NASA TN D-1406, 1962.

9. Hilsenrath, Joseph, et al.: Tables of Thermal Properties of Gases. National Bureau of Standards Circular 564, NBS, Nov. 1, 1955.

10. McAdams, William H.: Heat Transmission. Third ed., McGraw-Hill Book Co., Inc., 1954.

11. Coppage, J. E.: Heat Transfer and Flow Friction Characteristics of Porous Media. Tech. Rept. No. 16, Dept. Mech. Eng., Stanford Univ., Dec. 1, 1952.

12. London, A. L.; Mitchell, J. W.; and Sutherland, W. A.: Heat-Transfer and Flow-Friction Characteristics of Crossed-Rod Matrices. J. Heat Transfer (ASME Trans.), ser. C, vol. 82, no. 3, Aug. 1960, pp. 199-213.

13. Tong, L. S.; and London, A. L.: Heat-Transfer and Flow-Friction Characteristics of Woven-Screen and Crossed-Rod Matrices. ASME Trans., vol. 79, No. 7, Oct. 1957, pp. 1558-1570.

14. Morcom, A. R.: Fluid Flow Through Granular Materials. Trans. Inst. Chem. Engrs., vol. 24, Mar. 1946, p. 30.